

TESTING A NEW MONTE CARLO STRATEGY FOR FOLDING MODEL PROTEINS

HELGE FRAUENKRON¹, UGO BASTOLLA¹, ERWIN GERSTNER^{1,2},
PETER GRASSBERGER^{1,2}, AND WALTER NADLER¹

¹ *HLRZ c/o Forschungszentrum Jülich,
D-52425 Jülich, Germany*

² *Physics Department, University of Wuppertal,
D-42097 Wuppertal, Germany*

We demonstrate that the recently proposed pruned-enriched Rosenbluth method PERM (P. Grassberger, Phys. Rev. **E 56** (1997) 3682) leads to very efficient algorithms for the folding of simple model proteins. We test it on several models for lattice heteropolymers, and compare to published Monte Carlo studies of the properties of particular sequences. In *all* cases our method is faster than the previous ones, and in several cases we find new minimal energy states. In addition to producing more reliable candidates for ground states, our method gives detailed information about the thermal spectrum and, thus, allows to analyze static aspects of the folding behavior of arbitrary sequences.

1 Introduction

Protein folding^{1,2,3,4} is one of the most interesting and challenging problems in polymer physics and mathematical biology. It is concerned with the problem of how a heteropolymer of a given sequence of amino acids folds into precisely that geometrical shape in which it performs its biological function as a molecular machine.^{5,6} Currently, it is much simpler to find coding DNA—and, thus, also amino acid—sequences than to elucidate the 3-*d* structures of given proteins. Therefore, solving the protein folding problem would be a major break-through in understanding the biochemistry of the cell and, furthermore, in designing artificial proteins.

In this contribution we are concerned with the direct approach: given a sequence of amino acids, a molecular potential, and no other information, find the ground state and the equilibrium state at physiological temperatures. Note that we are not concerned with the kinetics of folding, but only in the final outcome. Also, we will not address the problems of how to find good molecular potentials,^{7,8,9} and what is the proper level of detail in describing proteins.⁸ Instead, we will use simple coarse-grained models which have been proposed in the literature and have become standards in testing the efficiency of folding algorithms.

Lots of methods have been proposed to solve this problem, ranging from simple Metropolis Monte Carlo simulations at some nonzero temperature¹⁰ over multi-canonical simulation approaches¹¹ to stochastic optimization schemes based, e.g., on simulated annealing,¹² and genetic algorithms.^{13,14} Alternative methods use heuristic principles,¹⁵ information from databases of known protein structures,¹⁶ sometimes in combination with known physico-chemical properties of small peptides.

The algorithms we apply here are variants of the pruned-enriched Rosenbluth method (PERM).¹⁷ This is a chain growth approach based on the Rosenbluth-Rosenbluth (RR)¹⁸ method. We will provide details on the algorithm and on the analyses that can be performed, and we will present more detailed results on ground

state and spectral properties, and on the folding behavior of the sequences analyzed.

2 The Models

The models we study in this contribution are heteropolymers that live on 2- and 3-dimensional regular lattices. They are self-avoiding chains with attractive or repulsive interactions between neighboring non-bonded monomers.

The majority of authors considered only two kinds of monomers. Although also different interpretations are possible for such a binary choice, e.g. in terms of positive and negative electric charges,¹⁹ the most important model of this class is the HP model.^{20,21} There, the two monomer types are assumed to be hydrophobic (H) and polar (P), with energies $\epsilon_{HH} = -1$, $\epsilon_{HP} = \epsilon_{PP} = 0$ for interaction between not covalently bound neighbors. Since this parameter set leads to highly degenerate ground states, alternative parameters were proposed, e.g. $\epsilon = (-3, -1, -3)$ ²² and $\epsilon = (-1, 0, -1)$.²³ Note, however, that in these latter parameter sets, since they are symmetric upon exchange of H and P, the intuitive distinction between hydrophilic and polar monomers gets lost.

In the other extremal case of models, all monomers of a sequence are considered to be different, and interaction energies are drawn randomly from a continuous distribution.^{24,25} These models correspond, effectively, to assuming an infinite number of monomer types.

3 The Algorithm

The algorithms we apply here are variants of the pruned-enriched Rosenbluth method (PERM),¹⁷ a chain growth algorithm based on the Rosenbluth-Rosenbluth (RR)¹⁸ method. Monomers are added sequentially, the n -th monomer being placed at site i with probability $p_n(i)$. In *simple sampling*, $p_n(i)$ is uniform on all neighbors of the last monomer, leading to exponential attrition. The original RR method avoids this by using a uniform $p_n(i)$ on all *vacant* neighbors of i_{n-1} . More generally, we call any non-uniform choice of $p_n(i)$ a generalized RR method. The relative thermal weight of a particular chain conformation of length n is then determined by $W_n = m_n \exp(-\beta \Delta E_n) W_{n-1}$, with $W_1 = 1$; ΔE_n is the energy gain from adding monomer n ; and m_n is the Rosenbluth factor, $m_n = \sum_{j \in \{\text{nn}\}} p_n(j)/p_n(i)$. We note that W_n is also an estimate for the partition function Z_n of the n -monomer chain.¹⁷ Chain growth is stopped when the final size is reached and started new from $n = 1$.

In easy cases, $p_n(i)$ can be chosen so that Boltzmann and Rosenbluth factors—or Rosenbluth factors for different n —cancel, leading to narrow weight distributions. But in general, this algorithm produces a wide spread in weights that can lead to serious problems.²⁶ On the other hand, since the weights accumulate as the chain grows, one can interfere during the growth process by ‘pruning’ conformations with low weights and enriching high-weight conformations. This is, in principle, similar to population based methods in polymer simulations^{27,28} and in quantum Monte Carlo (MC).²⁹ However, our implementation is different. Pruning is done stochastically: if the weight of a conformation has decreased below a threshold $W_n^<$, it is eliminated with probability 1/2, while it is kept and its weight is doubled in the other half of

cases. Enrichment³⁰ is done independently of this: if W_n increases above another threshold $W_n^>$, the conformation is replaced by n_c copies, each with weight W_n/n_c . Technically, this is done by putting onto a stack all information about conformations which still have to be copied. This is most easily implemented by recursive function calls.¹⁷ Thereby the need for keeping large populations of conformations^{27,28,29} is avoided. PERM has proven extremely efficient for studies of lattice homopolymers near the θ point,¹⁷ their phase equilibria,³¹ and of the ordering transition in semi-stiff polymers.³²

The main freedom when applying PERM consists in the a priori choice of the sites where to place the next monomer, in the thresholds $W^<$ and $W^>$ for pruning and copying, and in the number of copies made each time. All these features do not affect the formal correctness of the algorithm, but they can greatly influence its efficiency. They may depend arbitrarily on chain lengths and on local configurations, and they can be changed freely at any time during the simulation. Thus the algorithm can ‘learn’ during the simulation.

In order to apply PERM to heteropolymers at very low temperatures, the strategies proposed in Ref.¹⁷ are modified as follows.

(1) For homopolymers near the theta-point it had been found that the best choice for the placement of monomers was not according to their Boltzmann weights, but uniformly on all allowed sites.^{17,31} This might be surprising since the Boltzmann factor has then to be included into the weight of the configuration, which might lead to large fluctuations. Obviously, this effect is counterbalanced by the fact that larger Boltzmann factors correspond to higher densities and thus to smaller Rosenbluth factors.²⁶

For a heteropolymer this has to be modified, as there is no longer a unique relationship between density and Boltzmann factor. In a strategy of ‘anticipated importance sampling’ we should preferentially place monomers on sites with mostly attractive neighbors. Assume that we have two kinds of monomers, and we want to place a type- A monomer. If an allowed site has m_B neighbors of type B ($B = H, P$), we select this site with a probability $\propto 1 + a_{AH}m_H + a_{AP}m_P$. Here, a_{AB} are constants with $a_{AB} > 0$ for $\epsilon_{AB} < 0$ and vice versa.

(2) Most naturally, $W^>$ and $W^<$ are chosen proportional to the estimated partition sum Z_n .¹⁷ This becomes inefficient at very low T since Z_n will be underestimated as long as no low-energy state is found. When this finally happens, $W^>$ is too small. Thus too many copies are made which are all correlated but cost much CPU time.

This problem can be avoided by increasing $W^>$ and $W^<$ during particularly successful ‘tours’¹⁷ (a tour is the set of configurations derived from a single start). But then also the average number of long chains is decreased in comparison with short ones. To reduce this effect and to create a bias towards a sample which is flat in chain length, we multiply by some power of M_n/M_1 , where M_n is the number of generated chains of length n . With $\mathcal{N}(n)$ denoting the number of chains generated during the current tour we used therefore

$$W^< = C Z_n [(1 + \mathcal{N}(n)/M)(M_n + M)/(M_1 + M)]^2,$$

and $W^> = rW^<$. Here, C is a constant of order unity, $r \approx 10$, and M is a constant

of order $10^4 - 10^5$.

(3) Creating only one additional copy at each enrichment event (as done in Ref.¹⁷), cannot prevent the weights from exploding at very low T . Thus we have to make several copies if the weight is large and surpasses $W^>$ substantially. A good choice for the number of new copies created when $W > W^>$ is $\text{int}[1 + \sqrt{W/W^>}]$.

(4) Two special tricks were employed for ‘compact’ configurations of the 2- d HP model filling a square. First of all, since we know in this case where the boundary should be, we added a bias for polar monomers to actually be on that boundary, by adding an additional energy of -1 per boundary site. Note that this bias has to be corrected in the weights, thus the final distributions are unaffected by it and unbiased. Secondly, in two dimensions we can immediately delete chains which cut the free domain into two disjoint parts, since they never can grow to full length. In the present simulations, we checked for this by looking ahead one time step. In spite of the additional work this was very efficient, since it reduced considerably the time spent on dead-end configurations.

(5) In some cases we did not start to grow the chain from one end but from a point in the middle. We grew first one half, and then the other. Results were averaged over all possible starting points. The idea behind this is that real proteins have folding nuclei,³³ and it should be most efficient to start from such a nucleus. In some cases this trick was very successful and speeded up the ground state search substantially, in others not. We take this observation as an indication that in various sequences the end groups already provide effective nucleation sites. This is e.g. the case for the 80-mer with modified HP interactions of Ref.²³. We also tried to grow the chain on both sides simultaneously. However it turned out that this is not effective computationally.³⁴

(6) For an effective sampling of low-lying states the choice of simulation temperature T appears to be of importance. If it is too large, low-lying states will have a low statistical weight and will not be sampled reliably. On the other hand, if T is too low, the algorithm becomes too greedy: configurations which look good at first sight but lead to dead ends are sampled too often, while low energy configurations, whose qualities become apparent only at late stages of the chain assembly, are sampled rarely. Of course they then get huge weights (since the algorithm is correct after all), but statistical fluctuations become huge as well. This is in complete analogy to the slow relaxation hampering more traditional (Metropolis type) simulations at low T —note, however, that “relaxation” in the proper sense does not exist in the present algorithm.

In the cases we considered it turned out to be most effective to choose a temperature that is below the collapse transition temperature (note, however, that this transition is smeared out, see the results below) but somewhat above the temperature corresponding to the structural transition which leads to the native state. This observation corresponds qualitatively to the considerations of Ref.³⁵, although a quantitative comparison appears not to be possible. In some cases it also helped to reduce the ‘greediness’ of the algorithm by not making any pruning/enrichment during the first steps.

4 The Sequences

For the above models various sequences were analyzed in the literature, and in Ref.^{36,37} we took these analyses as a test for our algorithm. Here we will take a closer look at the properties of some of the sequences that were considered there.

4.1 2d HP model

Two-dimensional HP chains were used in several papers as test cases for folding algorithms. Two chains with $N = 100$ were studied in Ref.³⁸. The authors claimed that their native configurations were compact, fitting exactly into a 10×10 square, and had energies -44 and -46 , see Table 1 for the sequences and Fig. 1 and 2 for the respective proposed ground state structures. These conformations were found by a specially designed MC algorithm which should be particularly efficient for compact configurations.

4.2 3d HP model

Ten sequences of length $N = 48$ were given in Ref.³⁹. Each of these sequences was designed by minimizing the energy of a particular target conformation in sequence space under the constraint of constant composition.⁴⁰ The authors tried to find the

Table 1: Newly found lowest energy states for binary sequences with interactions $\epsilon = (\epsilon_{HH}, \epsilon_{HP}, \epsilon_{PP})$. Configurations are encoded as sequences of r (ight), l (eft), u (p), d (own), f (orward), and b (ackward).

N, d ϵ	sequence configuration	old $E_{\min}^{\text{Ref.}}$ new E_{\min}
100, 2 (-1, 0, 0)	$P_6HPH_2P_5H_3PH_5PH_2P_2(P_2H_2)_2PH_5PH_{10}-$	
	$PH_2PH_7P_{11}H_7P_2HPH_3P_6HPH_2$	-44^{38}
	$r_6ur_2u_3rd_5luldl_2drd_2ru_2r_3(rulu)_2urdrd_2ru_3lur_3dld_2-$	
	$ur_5d_3l_5uldl_2d_3ru_2r_3d_3l_2urul$	-47
	$rdldldrd_2r_2d_3l_2drldrd_2dl_2l_2(urul)_2urur_2ul_2u_2l_2drd_2-$	
	$lul_2urur_2r_2u_4rul_3drd_3l_2d_2ldl_2ru_2lu_3rd_2rdr$	-47
	$u_3r_3ur_5dl_4drd_2r_2ulur_4dr_2dl_2l_2ul_2ld_2rdl_2ul_3dr_2dr_2d-$	
	$rurdr_3d_2lul_2l_2drd_2lul_3l_2ul_2u_3ru$	-47
	$rdr_3dl_3drdrur_2ur_2ulur_2urd_2(ldrd)_2l_2u_2ldl_2dr_2dr_3dl_2d-$	
	$lulul_2ul_2d_3ldr_3u_2rdrldldrd_2urur_4u_3rul$	-47
100, 2 (-1, 0, 0)	$P_3H_2P_2H_4P_2H_3(PH_2)_3H_2P_8H_6P_2H_6P_9HPH_2PH_{11}-$	
	$P_2H_3PH_2PH_2HPH_3P_6H_3$	-46^{38}
	$ru_2ldlu_2ld_2lu_2lurulur_2d_2ru_4r_2dl_4ru_3rdrld_6rdru_3rul_2u_2-$	
	$rdr_2ulul_2(rd)_3rur_2dlld_4lul_2ru$	-49
	$u_3rdru_2rd_2ru_2r_2uldluldlu_5ld_6l_2d_2lu_3r_2u_6l_2d_3ldr_2dl_2-$	
	$dlul_2ru_2ldl_2drdl_2d_2rurdrd_3ru_3ru$	-49
	$ul_2drdl_2u_3ld_4ldr_2u_2l_2d_3l_2uru_3r_2u_3rd_3ru_4rul_5dlr_2-$	
	$d_2luldlrldlu_3lul_2ulur_2dr_2u_3rd_4l$	-49
	$r_3u_3ru_2ru_3l_2ur_2ul_2urul_4dr_2dlrld_2rur_2dl_2lul_2rdl_3-$	
	$uru_2ldld_3l_3urur_2rur_2ululdl_2u_3ld_4r$	-47
80, 3 (-1, 0, -1)	$PH_2P_3(H_3P_2H_3P_3H_2P_3)_3H_4P_4(H_3P_2H_3P_3H_2P_3)H_2$	$-94^{23,42}$
	$lbruflbl_2br_2drur_2dl_3ulfrdr_3urfldl_3ulurur_3drblul_3-$	
	$br_3bl_3dlrdr_3urul_2dlu$	-98

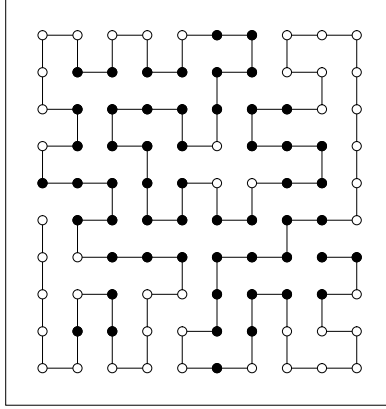


Figure 1: Putative compact native structure of sequence 1 from Table 1 ($E = -45$) according to Ref.³⁸; (filled circle) H monomers, (open circle) P monomers.

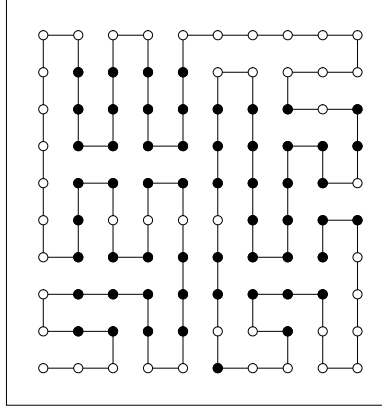


Figure 2: Putative compact native structure of sequence 2 from Table I ($E = -46$) according to Ref.³⁸.

lowest energy states with two different methods, one being an heuristic stochastic approach,¹⁵ the other based on exact enumeration of low energy states.⁴¹ With the first method they failed in all but one case to reach the lowest energy. With the second method in all but one cases they obtained conformations with energies that were even lower than the putative ground states the sequences were designed for, while for one case the ground state energy was confirmed. Precise CPU times were not quoted.

4.3 3d modified HP model

A most interesting case is a 2-species 80-mer with interactions $(-1, 0, -1)$ studied first in Ref.²³. These particular interactions were chosen instead of the HP choice $(-1, 0, 0)$ because it was hoped that this would lead to compact configurations. Indeed, the sequence was specially designed to form a “four helix bundle” which fits perfectly into a $4 \times 4 \times 5$ box, see Fig. 3. Its energy in this putative native state is $E = -94$. Although O’Toole *et al.*²³ used highly optimized codes, they were not able to recover this state by MC. Instead, they reached only $E = -91$. Supposedly, a different state with $E = -94$ was found in Ref.³⁸, but figure 10 of this paper, which is claimed to show this configuration, has a much higher value of E . Configurations with $E = -94$ but slightly different from that in Ref.²³ and with $E = -95$ were found in Ref.⁴² by means of an algorithm similar to that in Ref.³⁸. For each of these low energy states the author needed about one week of CPU time on a Pentium.

4.4 3d, infinitely many monomer types

Sequences with $N = 27$ and with continuous interactions were studied by Klimov *et al.*²⁵. Interaction strengths were sampled from Gaussians with fixed non-zero mean and fixed variance. These $N(N - 1)/2$ numbers were first attributed randomly to

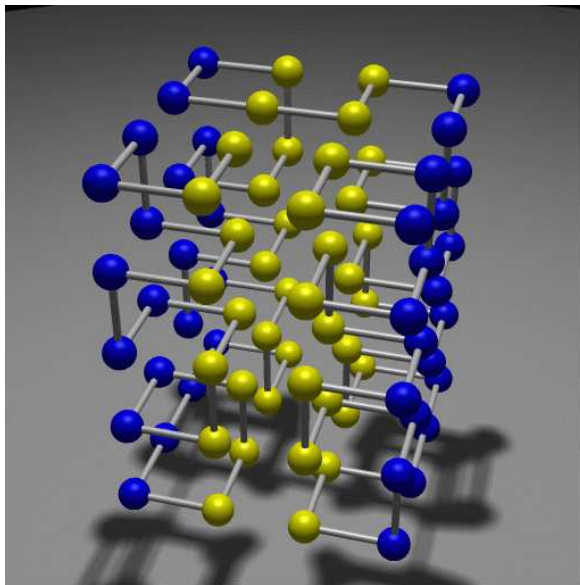


Figure 3: Putative native state of the “four helix bundle” sequence, see Table 1, as proposed by O’Toole *et al.*. It has $E = -94$, fits into a rectangular box, and consists of three homogeneous layers. Structurally, it can be interpreted as four helix bundles.

the monomer pairs, then they were randomly permuted, using a Metropolis accept/reject strategy with a suitable cost function, to obtain good folders. Such “breeding” strategies to obtain good folders were also developed and employed by other authors for various models,^{40,43,44} and seem necessary to eliminate sequences which fold too slowly and/or unreliably. It is believed that also during biological evolution optimization processes took place with similar effects, so that actual proteins are better folders than random amino sequences.

5 Results

Let us now discuss our results. All CPU times quote below refer to SPARC Ultra machines with 167 MHz.

5.1 2d HP model

For the two HP chains of Ref.³⁸ with $N = 100$, see Table 1, we found several compact states (within ca. 40 hours of CPU time) that had energies lower than those of the compact putative ground states proposed in Ref.³⁸. Figures 4 and 5 show representative compact structures with $E = -46$ for sequence 1 and $E = -47$ for sequence 2. Moreover, we found several non-compact configurations with energies even lower: the lowest energies found within 1–2 days of CPU time had $E = -47$ and $E = -48$ for sequence 1 and 2, respectively. Forbidding non-bonded HP pairs, we obtained even $E = -49$ for sequence 2. Figures 6 and 7 show representative non-

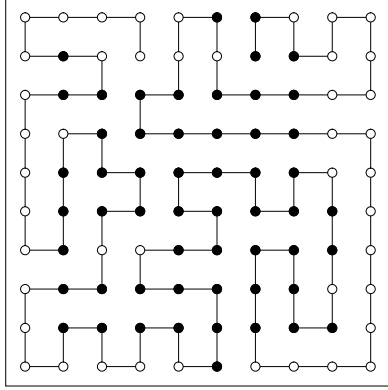


Figure 4: One of the compact structures of sequence 1 with energy ($E = -46$) lower than the “native” state proposed by Ramakrishnan *et al.*³⁸.

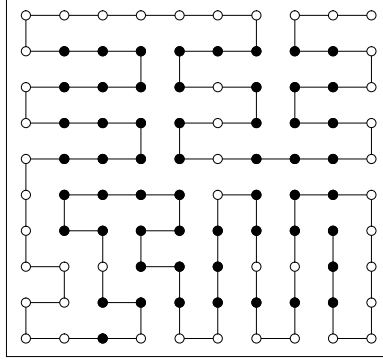


Figure 5: One of the compact structures of sequence 2 with lower energy ($E = -47$).

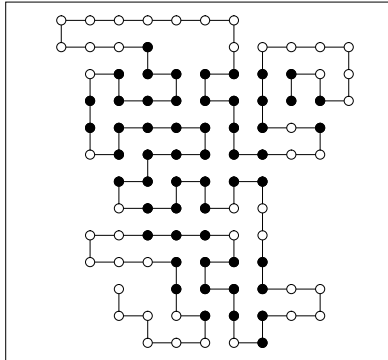


Figure 6: One of the (non-compact) lowest energy sequences for sequence 1 ($E = -47$).

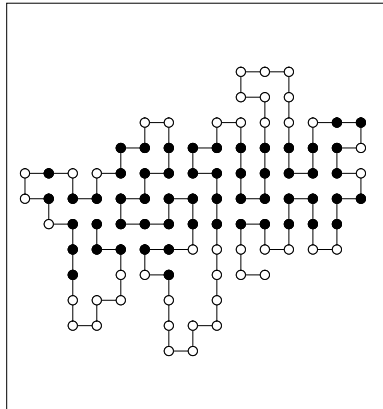


Figure 7: One of the (non-compact) lowest energy sequences for sequence 2 ($E = -49$).

compact structures with these energies; a non-exhaustive collection of these is listed in Table 1. These results reflect the well-known property that HP sequences (and those of other models) usually have ground states that are not maximally compact, see, e.g. Yue *et al.*³⁹, although there is a persistent prejudice to the contrary.^{23,38,45}

5.2 3d HP model

With PERM we succeeded to reach ground states of the ten sequences of length $N = 48$ given in Ref³⁹ in *all* cases, in CPU times between a few minutes and one day, see Table 2. In these simulations we used a rather simple version of PERM, where we started assembly always from the same end of the chain. We found that the sequences most difficult to fold were also those which had resisted previous Monte Carlo attempts.³⁹ In those cases where a ground state was hit more than

Table 2: PERM performance for the binary sequences from Ref.³⁹

sequence nr.	$-E_{\min}^a$	$-E_{\text{MC}}^b$	n_{success}^c	CPU time (min)
1	32	31	101	6.9
2	34	32	16	40.5
3	34	31	5	100.2
4	33	30	5	284.0
5	32	30	19	74.7
6	32	30	24	59.2
7	32	31	16	144.7
8	31	31	11	26.6
9	34	31	1	1420.0
10	33	33	16	18.3

^a Ground state energies.³⁹

^b Previously reached energies with Monte Carlo methods.³⁹

^c Number of independent tours in which a ground state was hit.

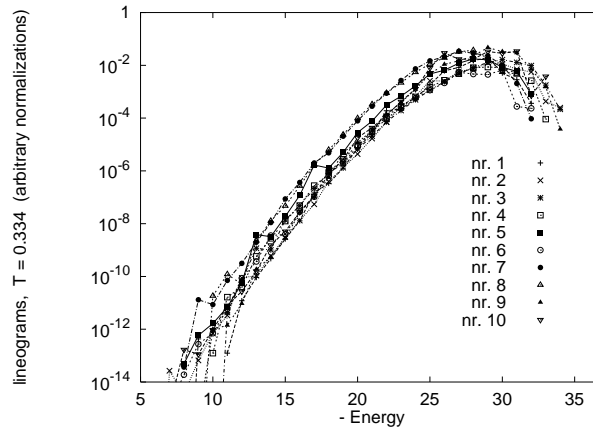


Figure 8: Energy spectrum of the ten sequences given in Ref.³⁹. More precisely, to emphasize the low-energy part of the spectrum, we show the histograms obtained from the spectra by multiplying with $e^{E/T}$, $T = 0.334$. Note that there are no energy gaps in any of these spectra.

once, we verified also that the ground states were highly degenerate. In no case there were gaps between ground and first excited states, see Fig. 8. Therefore, none of these sequences is a good folder, though they were designed specifically for this purpose.

5.3 3d modified HP model

For the two-species 80-mer with interactions $(-1, 0, -1)$, even without much tuning our algorithm gave $E = -94$ after a few hours, but it did not stop there. After a number of rather disordered configurations with successively lower energies, the final candidate for the native state has $E = -98$. It again has a highly symmetric

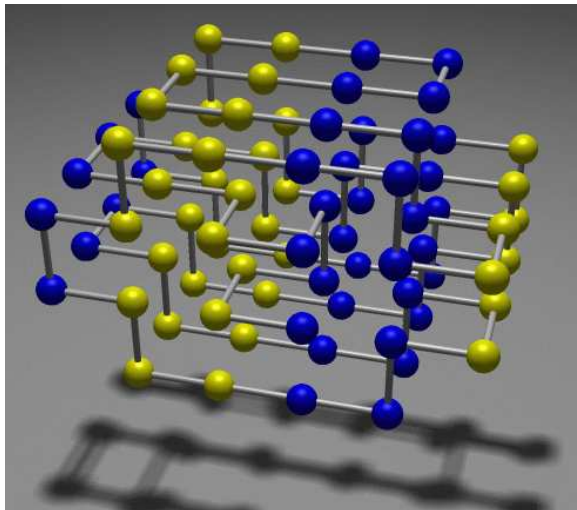


Figure 9: Conformation of the “four helix bundle” sequence with $E = -98$. We propose that this is the actual ground state. Its shape is highly symmetric although it does not fit into a rectangular box. It is not degenerate except for a flipping of the central front $2 \times 2 \times 2$ box.

shape, although it does not fit into a $4 \times 4 \times 5$ box, see Fig. 9. It has twofold degeneracy (the central $2 \times 2 \times 2$ box in the front of Fig. 9 can be flipped), and both configurations were actually found in the simulations. Optimal parameters for the ground state search in this model are $\beta = 1/kT \approx 2.0$, $a_{PP} = a_{HH} \approx 2$, and $a_{HP} \approx -0.13$. With these, average times for finding $E = -94$ and $E = -98$ in new tours are ca. 20 min and 80 hours, respectively.

A surprising result is that the monomers are arranged in four homogeneous layers in Fig. 9, while they had formed only three layers in the putative ground state of Fig. 3. Since the interaction should favor the segregation of different type monomers, one might have guessed that a configuration with a smaller number of layers should be favored. We see that this is outweighed by the fact that both monomer types can form large double layers in the new configuration. Again, our new ground state is not ‘compact’ in the sense of minimizing the surface, and hence it also disagrees with the wide spread prejudice that native states are compact.

In terms of secondary structure, the new ground state is fundamentally different from the putative ground state of Ref.³⁸. While the new structure (Fig. 9) is dominated by β sheets, which can most clearly be seen in the contact matrix (see Fig. 10), the structure in Fig. 3 is dominated by helices, see also the corresponding contact matrix in Fig. 11.

In order to analyze the folding transition of this sequence we again constructed histograms of the distribution of energy, end to end distance, and radius of gyration, by combining the results obtained at various temperatures between $T = 0.45$ and 3. Figure 12 shows these distributions, reweighted so that it corresponds to $T = 0.75$. The thermal behavior of these order parameters as functions of T is obtained by Laplace transform, and is shown in Fig. 13. The behavior of energy, end-to-end dis-

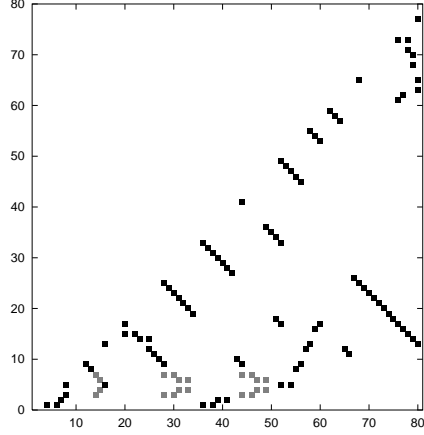


Figure 10: Contact matrix of the structure in Fig. 9; a black point at (i, j) indicates that there is a contact between monomer i and monomer j ; grey points indicate contacts in only one of the two native states, corresponding to the twofold degeneracy of the central $2 \times 2 \times 2$ box. Note that the lines orthogonal to the main diagonal correspond to anti-parallel β -sheet secondary structure elements, see e.g. Ref.⁴⁶.

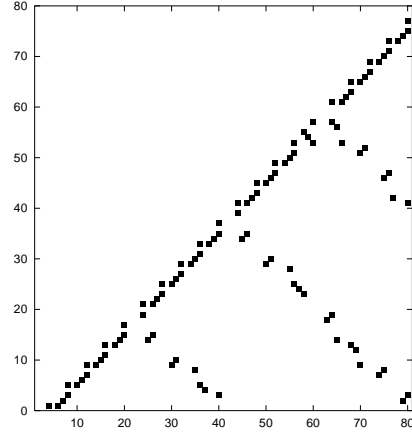


Figure 11: For comparison, the contact matrix of the putative ground state of Ref.³⁸ in Fig. 3; note that point triples close to the diagonal parallel as well as orthogonal to it are signatures of 3d helical secondary structure elements, see e.g. Ref.⁴⁶; the other points denote tertiary contacts between helices.

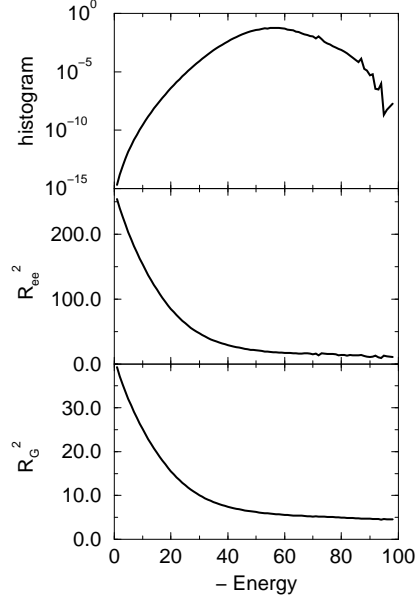


Figure 12: Histograms of (top) thermal weight, (middle) radius of gyration, R_G^2 , and (bottom) end-to-end distance, R_{ee}^2 , vs energy E for the 80-mer “four helix bundle” at $T = 0.75$.

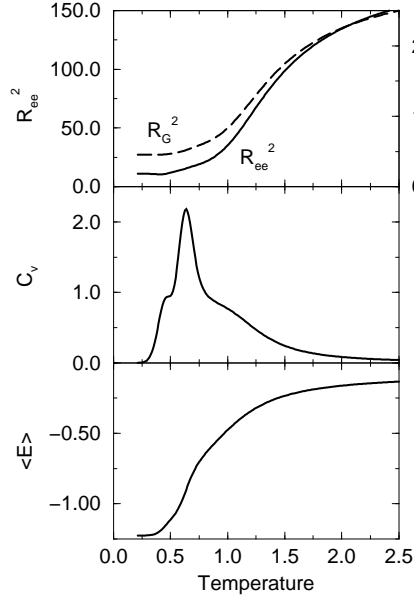


Figure 13: (top) Average end-to-end distance, R_{ee}^2 , and radius of gyration, R_G^2 , (middle) specific heat per monomer, C_v , and average energy per monomer, $\langle E \rangle$, vs temperature T for the 80-mer “four helix bundle”.

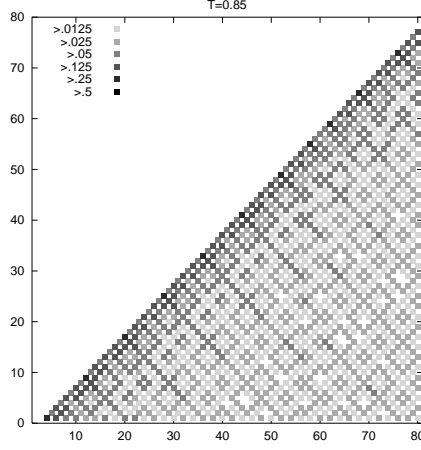


Figure 14: Thermally averaged contact matrix for the 80-mer “four helix bundle” in the collapsed but unstructured phase ($T = 0.85$).

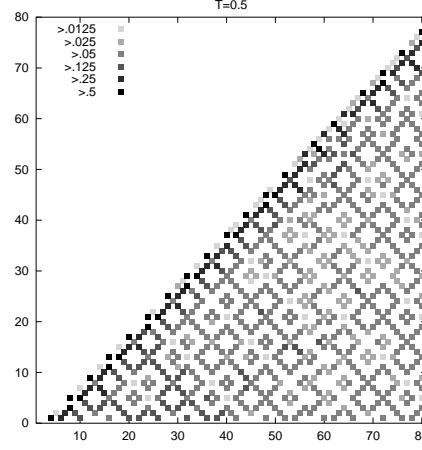


Figure 15: Thermally averaged contact matrix for the 80-mer “four helix bundle” in the intermediate helix-dominated phase ($T = 0.5$).

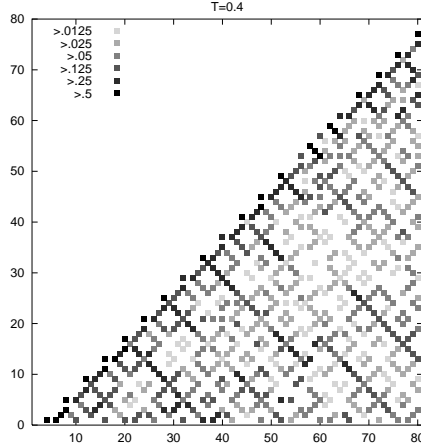


Figure 16: Thermally averaged contact matrix for the 80-mer “four helix bundle” at the transition from the intermediate helix-dominated to the β -sheet dominated phase ($T = 0.4$).

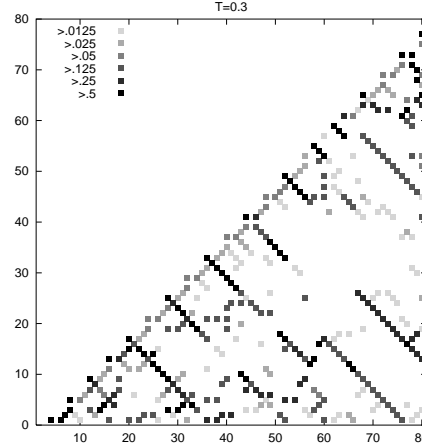


Figure 17: Thermally averaged contact matrix for the 80-mer “four helix bundle” in the β -sheet dominated phase ($T = 0.3$).

tance and radius of gyration follow closely each other and exhibit only the smeared out collapse of the chain from a random coil to some unstructured compact phase. In contrast, the specific heat exhibits more structure: the shoulder around $T = 1$ corresponds again to the coil-globule collapse, but there are additional transitions seen around $T = 0.62$ and $T = 0.45$. The last one is the transition to the β -sheet dominated native phase. However, the transition at $T = 0.62$ is from a unstructured globule to an intermediate phase that is helix-dominated but exhibits strong tertiary fluctuations. These structural transitions are illustrated in Figs 14 to 17 where the thermally averaged contact matrices are shown for the respective phases.

The intermediate, helix-dominated phase is particularly interesting. To it apply

some of the usual characteristics of a molten globule state⁴⁷: i) compactness, ii) large secondary structure content (although not necessarily native), and iii) strong fluctuations.

5.4 3d, infinitely many monomer types

For all sequences with $N = 27$ from Ref.²⁵ we could reach the supposed ground state energies within < 1 hour. In no case we found energies lower than those quoted in Ref.²⁵, and we verified also the energies of low-lying excited states given in Ref.²⁵. Notice that these sequences were designed to be good folders by Klimov *et al.*²⁵. This time the design had obviously been successful, which is mainly due to the fact that the number of different monomer types is large. All sequences showed some gaps between the ground state and the bulk of low-lying states, although these gaps are not very pronounced in some cases.

More conspicuous than these gaps was another feature: all low lying excited states were very similar to the ground state, as measured by the fraction of contacts which existed also in the native configuration. Stated differently, if the gaps were not immediately obvious, this was because they were filled by configurations which were very similar to the ground state and can therefore easily transform into the native state and back. Such states therefore cannot prevent a sequence from being a good folder. For none of the sequences of Ref.²⁵ we found truly misfolded low-lying states with small overlap with the ground state.

Figure 18 illustrates this feature for one particular sequence. There we show the *overlap* Q , defined as the fraction by non-bonded nearest-neighbor ground state contacts which exist also in the excited state, against the excitation energy. For this and for each of the following figures, the 500 lowest-lying states were determined. We see no low energy state with a small value of Q . To demonstrate that this is due to design, and is not a property of random sequences with the same potential distribution, we show in Fig. 19 the analogous distribution for a random sequence.

To demonstrate that this difference is not merely due to a statistical fluctuation,

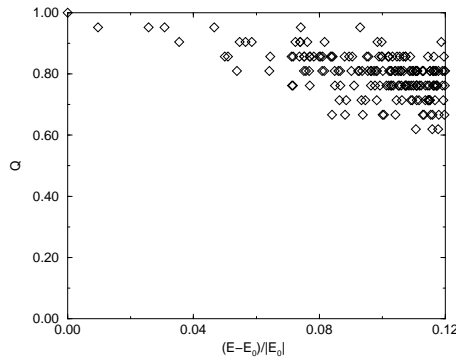


Figure 18: Overlap with ground state, Q , vs energy, E , of the lowest energy conformations for sequence no. 70 of Ref.²⁵.

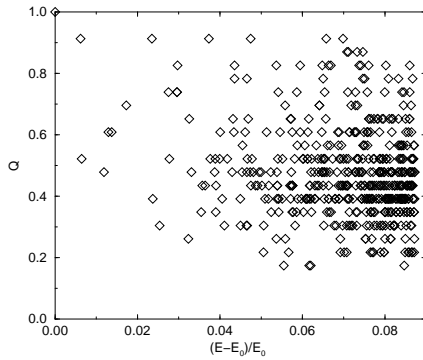


Figure 19: Overlap with ground state, Q , vs energy, E , of the lowest energy conformations for a single random sequence.

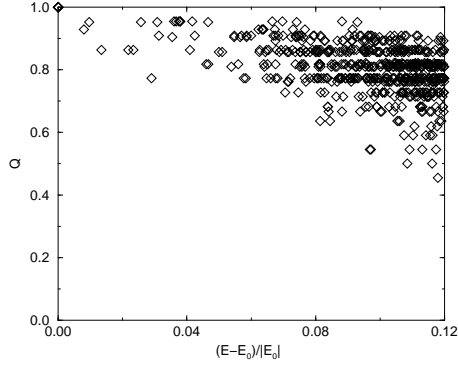


Figure 20: Overlap with ground state, Q , vs energy, E , of the lowest energy conformations for sequences no. 61 to 70 of Ref.²⁵; for better visibility, the same symbol is used for all sequences.

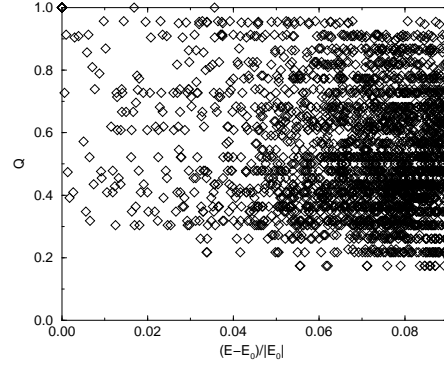


Figure 21: Overlap with ground state, Q , vs energy, E , of the lowest energy conformations for ten random sequences; for better visibility, the same symbol is used for all sequences.

we show in Fig. 20 the distributions for ten sequences from Ref.²⁵ collected in a single plot. Since the ground state energies differ considerably for different sequences, we used normalized excitation energies $(E - E_0)/E_0$ on the x-axis. Analogous results for ten random sequences are shown in Fig. 21. While there is no obvious correlation between Q and excitation energies for the random case, all low energy states with small Q have been eliminated in the designed sequences.

This elimination of truly misfolded low energy states without elimination of native-like low energy states might be an unphysical property of the design procedure used in Ref.²⁵, but we do not believe that this is the case. Rather, it should be a general feature of any design procedure, including the one due to biological evolution. It contradicts the claim of Ref.²⁴ that it is only the gap between native and first excited state which determines foldicity. On the other hand, our results are consistent with the “funnel” scenario for the protein folding process,⁴⁸ where the folding pathway consists of states successively lower in energy and closer to the native state.

We note that for random sequences there are also excited states that have unit overlap with the native state, a feature not present in the folding sequences. These are cases where the native state has open loops and/or dangling ends, so that more compact conformations have all contacts of the native state, but have—in addition—energetically unfavorable contacts resulting in a higher total energy.

6 Summary and Outlook

We showed that the pruned-enriched Rosenbluth method (PERM) can be very effectively applied to protein structure prediction in simple lattice models. It is suited for calculating statistical properties and is very successful in finding native states. In all cases it did better than any previous MC method, and in several cases it found lower energy states than those which had previously been conjectured to

be native.

We verified that ground states of the HP model are highly degenerate and have no gap, leading to bad folders. For sequences that are good folders we have established a funnel structure in state space: low-lying excited states of well-folding sequences have strong similarities to the ground state, while this is not true for non-folders with otherwise similar properties.

Especially, we have presented a new candidate for the native configuration of a “four helix bundle” sequence which had been studied before by several authors. The ground state structure of the “four helix bundle” sequence, being actually β -sheet dominated, differs strongly from the helix-dominated intermediate phase. This sequence, therefore, should not be a good folder.

Although we have considered only lattice models in this paper, we should stress that this is not an inherent limitation of PERM. Straightforward extensions to off-lattice systems are possible and are efficient for homopolymers at relatively high temperatures.¹⁷ Recently performed simulations of a 2-dimensional off-lattice protein model⁴⁹ have shown that PERM is not quite as fast as the *simulated tempering*⁵⁰ algorithm used by Irbäck *et al.*⁴⁹. But there are several ways to improve PERM. One way could be to adopt a strategy similar to simulated tempering. Another improvement of PERM which could be particularly useful for off-lattice simulations might consist in more sophisticated algorithms for positioning the monomers when assembling the chain. In particular one might try to use some feedback of successfully build up low energy states or subchains for the positioning of previous monomers in the following tours. Finally, one can use configurations reached by PERM as a starting point for alternative (Metropolis or greedy) searches. Work along these lines is in progress, and we hope to report on it soon.

Acknowledgments

The authors are grateful to Gerard Barkema for helpful discussions during this work. One of them (P.G.) wants to thank also Eytan Domany and Michele Vendruscolo for very informative discussions, and to Drs. D.K. Klimov and R. Ramakrishnan for correspondence.

References

1. L. M. Gierasch and J. King (eds.), *Protein Folding, Deciphering the Second Half of the Genetic Code* (AAAS, New York, 1990)
2. T.E. Creighton (ed.), *Protein Folding* (Freeman, New York, 1992)
3. K. M. Merz Jr. and S. M. LeGrand (eds.), *The Protein Folding Problem and Tertiary Structure Prediction* (Birkhäuser, Boston, 1994)
4. H. Bohr and S. Brunak (eds.), *Protein Folds: A Distance Based Approach* (CRC Press, Boca-Raton/FL, 1996).
5. K. E. Drexler, *Engines of Creation*, (Anchor Books, 1986); available also on the web at the URL <http://www.asiapac.com/EnginesOfCreation/>.
6. M. Groß, *Expeditionen in den Nanokosmos*, (Birkhäuser, Basel, 1995).
7. G. M. Crippen and V. N. Maiorov, in Ref.³, p.231–277.

8. A. Kolinski and J. Skolnick, *Lattice Models of Protein Folding, Dynamics and Thermodynamics*, (Chapman & Hall, New York, 1996).
9. L. A. Mirny and E. I. Shakhnovich, J. Mol. Biol. **264**, 1164 (1996).
10. A. Sali, E. I. Shakhnovich and M. Karplus J. Mol. Biol. **235**, 1614 (1994).
11. U. H. E. Hansmann and Y. Okamoto, J. Comp. Chem. **14**, 1333 (1993); Physica A **212**, 415 (1994); Phys. Rev. E **54**, 5863 (1996).
12. S. R. Wilson and W. Cui, in Ref.³, p.43–70.
13. R. Unger and J. Moult, J. Mol. Biol. **231**, 75 (1993)
14. S. M. LeGrand and K. M. Merz jr., in Ref.³, p.109–124.
15. K. A. Dill, K. M. Fiebig and H. S. Chan, Proc. Natl. Acad. Sci USA **90**, 1942 (1993).
16. F. Eisenhaber, B. Persson and P. Argos, Crit. Rev. Biochem. Mol. Biol. **30**, 1 (1995).
17. P. Grassberger, Phys. Rev. E **56**, 3682 (1997).
18. M.N. Rosenbluth and A.W. Rosenbluth, J. Chem. Phys. **23**, 256 (1955)
19. Y. Kantor and M. Kardar, Europhys. Lett. **28**, 169 (1994)
20. K.A. Dill, Biochemistry **24**, 1501 (1985)
21. K.F. Lau and K.A. Dill, Macromolecules **22**, 3986 (1989); J. Chem. Phys. **95**, 3775 (1991); H.S. Chan, and K.A. Dill, J. Chem. Phys. **95**, 3775 (1991)
22. N.D. Socci and J.N. Onuchic, J. Chem. Phys. **101**, 1519 (1994)
23. E. O'Toole and A. Panagiotopoulos, J. Chem. Phys. **97**, 8644 (1992)
24. A. Sali, E. I. Shakhnovich and M. Karplus, Nature **369** 248 (1994).
25. D.K. Klimov and D. Thirumalai, Proteins: Structure, Function and Genetics **26**, 411 (1996); sequences available from <http://www.glue.umd.edu/~klimov>
26. J. Batoulis and K. Kremer, J. Phys. A **21**, 127 (1988)
27. T. Garel and H. Orland, J. Phys. A **23**, L621 (1990)
28. B. Velikson, T. Garel, J.-C. Niel, H. Orland and J.C. Smith, J. Comput. Chem. **13**, 1216 (1992)
29. C.J. Umrigar, M.P. Nightingale, and K.J. Runge, J. Chem. Phys. **99**, 2865 (1993)
30. F.T. Wall and J.J. Erpenbeck, J. Chem. Phys. **30**, 634, 637 (1959)
31. H. Frauenkron and P. Grassberger, J. Chem. Phys. **107**, 9599 (1997)
32. U. Bastolla and P. Grassberger, J. Stat. Phys. **89**, 1061 (1997)
33. R. R. Matheson and H. A. Scheraga, Macromolecules **11**, 819 (1978).
34. At first sight, one might believe that allowing the chain to grow at both ends should decrease the attrition rate and hence be advantageous. For homopolymers one can see easily that this is not true. Attrition is actually decreased, since chains which have one end blocked can still grow at the other end. But such chains have small Rosenbluth factors and thus extremely low W in average. Therefore, they just cost efforts without efficiently contributing to statistical averages. For heteropolymers this argument no longer holds, however, and it is not clear why growing the chain at both ends is not efficient either.
35. A. V. Finkelstein, A. M. Gutin and A. Y. Badretidinov PROTEINS: Structure, Function and Genetics **23**, 151 (1995).
36. H. Frauenkron, U. Bastolla, E. Gerstner, P. Grassberger and W. Nadler, Phys.

- Rev. Lett. **80**, 3149 (1998).
37. U. Bastolla, H. Frauenkron, E. Gerstner, P. Grassberger and W. Nadler, to appear in PROTEINS (1998).
 38. R. Ramakrishnan, B. Ramachandran and J.F. Pekney, J. Chem. Phys. **106**, 2418 (1997)
 39. K. Yue *et al.*, Proc. Natl. Acad. Sci. USA **92**, 325 (1995)
 40. E. I. Shakhnovich and A. M. Gutin, Proc. Natl. Acad. Sci USA **90**, 7195 (1993); E. I. Shakhnovich, Phys. Rev. Lett. **72**, 3907 (1994).
 41. K. Yue and K. A. Dill, Proc. Natl. Acad. Sci USA **92**, 146 (1995).
 42. J.M. Deutsch, J. Chem. Phys. **106**, 8849 (1997).
 43. M. Ebeling and W. Nadler, Proc. Natl. Acad. Sci. USA **92**, 8798 (1995); Biopolymers **41**, 165 (1997).
 44. J.M. Deutsch and T. Kurosky, Phys. Rev. Lett. **76**, 323 (1996).
 45. E. I. Shakhnovich and A. M. Gutin, J. Chem. Phys. **93**, 5967 (1990); A. M. Gutin and E. I. Shakhnovich, J. Chem. Phys. **98**, 8174 (1993).
 46. H. S. Chan and K. A. Dill, Macromolecules **22**, 4559 (1989); J. Chem. Phys. **92**, 3118 (1990).
 47. H. Christensen and R. H. Pain, Europ. Biophys. J. **19**, 221 (1991).
 48. P. G. Wolynes, J. N. Onuchic, and D. Thirumalai, Science **267**, 1619 (1995).
 49. A. Irbaeck, C. Peterson and F. Potthast, J. Phys. Rev. **E 55**, 860 (1997).
 50. E. Marinari and G. Parisi, Europhys. Lett. **19**, 451 (1992).